

# Point information gain, point information gain entropy and point information gain entropy density as measures of semantic and syntactic information of multidimensional discrete phenomena

Renata Rychtáriková, Jan Korbel, Petr Macháček, Petr Císař, Jan Urban, Dmytro Soloviov and Dalibor Štys

## Abstract

We generalize the point information gain (PIG) and derived quantities, i.e., point information gain entropy (PIE) and point information gain entropy density (PIED), for the case of the Rényi entropy and simulate the behavior of PIG for typical distributions. We also use these methods for the analysis of multidimensional datasets. We demonstrate the main properties of PIE/PIED spectra for the real data on the example of several images, and discuss further possible utilizations in other fields of data processing.

## Index Terms

Point information gain, Rényi entropy, Data processing

## I. INTRODUCTION

Measurement of relative information between two probability distributions is one of the most important goals of information theory. Among many other concepts, there are two, which are widely used. By far the most widespread concept is called relative Shannon entropy or Kullback–Leibler divergence. In this work, we rather use an alternative

Renata Rychtáriková, Petr Macháček, Petr Císař, Jan Urban, Dmytro Soloviov, Dalibor Štys are with Institute of Complex Systems, South Bohemian Research Center of Aquaculture and Biodiversity of Hydrocenoses, FFPW, University of South Bohemia in České Budějovice, Zámek 136, 373 33 Nové Hradky, Czech Republic (email: stys@frov.jcu.cz). This work was supported by Postdok JU CZ.1.07/2.3.00/30.0006, the GAJU 134/2013/Z, TA CR TA01010214, and the Ministry of Education, Youth and Sports of the Czech Republic projects CENAKVA (No. CZ.1.05/2.1.00/01.0024) and CENAKVA II (No. LO1205 under the NPU I program).

Jan Korbel is with Faculty of Nuclear Sciences and Physical Engineering, Czech Technical University in Prague, Břehová 7, 155 19, Prague, Czech Republic and acknowledges the support from GAČR, Grant No. GCP402/12/J077.

approach based on a simple concept of entropy difference. By generalization of both concepts from Shannon's approach to Rényi's approach we obtain the whole class of information measures that enables to aim to different parts of probability distributions and interpret it as investigation of different parts of multifractal systems.

Despite the mathematical precision of the concept of Shannon/Rényi divergence, we use the latter concept, i.e., (Rényi) entropy difference, for introduction of a measure which locally determines an information contribution of a given element in a discrete set. In spite of no substantial restriction on the use of a standard divergence for calculation of the information difference upon elimination of one element from the set, for practical reasons, we used a simple concept of entropy difference between sets with and without a given element. The resulting value has been called the point information gain  $\Gamma_{\alpha,i}$  [1], [2]. The goal of this article is to examine and demonstrate some properties of this variable and derived quantities, namely a point information gain entropy  $H_\alpha$  and point information gain entropy density  $\Xi_\alpha$ . We also introduce the relation of all these variables to semantic and syntactic information in multidimensional data analysis.

## II. POINT INFORMATION GAIN, POINT INFORMATION GAIN ENTROPY, AND POINT INFORMATION GAIN ENTROPY DENSITY AND THEIR PROPERTIES

### A. Point information gain and its relation to other information entropies

The important problem in the information theory is to estimate the amount of information gained/lost by refining/approximating the probability distribution  $P$  by distribution  $Q$ . The most popular measure used in the theory is Kullback-Leibler (KL) divergence, defined as

$$D_{KL}(P||Q) = \sum_i p_i \ln \frac{p_i}{q_i} = E_p [\ln q_i] - E_p [\ln p_i] = S_P(Q) - S(P), \quad (1)$$

where  $S_P(Q)$  is so-called cross-entropy [3] and  $S(P)$  is the entropy of distribution  $P$ . In case, when  $P$  is similar to  $Q$ , this measure can be approximated by entropy difference

$$\Delta S(P, Q) = S(Q) - S(P). \quad (2)$$

Indeed, this measure does not obey as many theoretic-measure axioms as KL-divergence. For instance, for  $P \neq Q$  we can still obtain  $|\Delta S(P, Q)| = 0$ . Nevertheless, if  $P \approx Q$  and  $P \neq Q$ , this measure can be still a suitable information measure. The situation, when the distributions are approximative histograms of some underlying distributions  $P$  for  $n$  and  $n + 1$  entries, respectively, is particularly interesting. In this case, the entropy difference

$$\Delta S(P_n, P_{n+1}) = S(P_{n+1}) - S(P_n) \quad (3)$$

can be interpreted as an information gained by the  $(n + 1)$ -th point.

When dealing with complex real systems, it is sometimes advantageous to introduce new information measures and entropies that capture the complexity of the system better – e.g., Hellinger distance, Jeffrey's distance or J-divergence. There are also some specific information measures that have special interpretations and are widely used in various applications. The two most important measures are the Tsallis-Havrda-Charvát (THC) entropy [4], which is the entropy of non-extensive systems, and the Rényi entropy, the entropy of multifractal systems [5], [6]. The

latter one is tightly connected to theory of multifractal systems and generalized dimensions [7], the scaling exponent of the Rényi entropy

$$\mathcal{H}_\alpha(P) = \frac{1}{\alpha - 1} \ln \sum_i p_i^\alpha \quad (4)$$

is equal to the generalized dimension  $D_\alpha = \lim_{l \rightarrow 0} \frac{\mathcal{H}_\alpha(P(l))}{\ln l}$ . Rényi entropy indicates the average information cost, when the cost of information is an exponential function of its length [8]. Thus, changing the parameter  $\alpha$  changes the cost of the information and therefore accentuates some parts of the probability distributions while suppressing the other. The limit  $\lim_{\alpha \rightarrow 1} \mathcal{H}_\alpha = \mathcal{H}_1$  is equal to the Shannon entropy, thus, by taking into account the whole class of Rényi entropies, we get a new class of information measures.

The point information gain  $(\Gamma_{\alpha, i})$  was developed as a practical tool for assessment of information contribution of an element to a given discrete distribution [9]. Similarly to Shannon's entropy difference, it is defined as a difference of two Rényi entropies – with and without the examined element of a discrete phenomenon. We consider a discrete distribution of  $k$  phenomena, which occur exclusively. The  $\mathcal{H}_\alpha = \mathcal{H}_\alpha(P)$  is the Rényi entropy of the full distribution and  $\mathcal{H}_{\alpha, i} = \mathcal{H}_\alpha(P_i)$  is the Rényi entropy of the distribution  $P_i$ , in which one point in the occurrence of the examined  $i$ -th phenomenon was omitted. Hence, we may write the point information gain  $\Gamma_{\alpha, i}$  as

$$\Gamma_{\alpha, i} = \mathcal{H}_{\alpha, i} - \mathcal{H}_\alpha = \frac{1}{1 - \alpha} \ln \left( \sum_{j=1}^k p_{j, i}^\alpha \right) - \frac{1}{1 - \alpha} \ln \left( \sum_{j=1}^k p_j^\alpha \right) = \frac{1}{1 - \alpha} \ln \left( \frac{\sum_{j=1}^k p_{j, i}^\alpha}{\sum_{j=1}^k p_j^\alpha} \right), \quad (5)$$

where  $\alpha$  is the Rényi coefficient,  $k$  is the number of elements in the discrete distribution,  $p_j = n_j/n$  and  $p_{j, i} = n_{j, i}/(n-1)$  is the probability of occurrence of the  $j$ -th phenomenon in the original distribution and in the distribution without one element of the  $i$ -th phenomenon, respectively<sup>1</sup>.

In contrast to the commonly used Rényi divergence [10]–[16], we use  $\Gamma_{\alpha, i}$  for its relative simplicity<sup>2</sup> and practical interpretation.

After the substitution for probabilities, one gets that

$$\Gamma_{\alpha, i} = \frac{1}{1 - \alpha} \ln \frac{\sum_{j=1}^k \frac{n_{j, i}^\alpha}{(n-1)^\alpha}}{\sum_{j=1}^k \frac{n_j^\alpha}{n^\alpha}} = \mathcal{C}_\alpha(n) + \frac{1}{1 - \alpha} \ln \frac{\sum_{j=1}^k n_{j, i}^\alpha}{\sum_{j=1}^k n_j^\alpha}, \quad (6)$$

where  $\mathcal{C}_\alpha(n) = \frac{1}{1 - \alpha} \ln \frac{n^\alpha}{(n-1)^\alpha}$  is depending only on the number of events  $n$ . For  $n \rightarrow \infty$ ,  $\Gamma_{\alpha, i} \rightarrow 0$ , and the whole entropy remains finite<sup>3</sup>. Therefore, we examine only the second term. When the argument of the logarithm is close to 1, e.g.,

$$\sum_{j=1}^k n_{j, i}^\alpha \approx \sum_{j=1}^k n_j^\alpha, \quad (7)$$

<sup>1</sup>From technical point of view, in the mathematical part of the text we have used the natural logarithm in order to simplify the deduction. However, all calculations have been performed with the usage of  $\log_2$  which, for Rényi entropy and its derivatives, yields values in bits.

<sup>2</sup>Unlike KL divergence, Rényi divergence cannot be interpreted as a difference of cross-entropy and entropy of underlying distribution.

<sup>3</sup>contrary to unconditional entropy, which has to be renormalized for continuous case, for details see Ref. [5]

which leads to the condition that  $\left(\frac{n_i-1}{n_i}\right)^\alpha \approx 1$ , one can then approximate the logarithm by the Taylor expansion of the first order. By denoting

$$\mathcal{D}_{\alpha,i} = \frac{\sum_{j=1}^k n_{j,i}^\alpha}{\sum_{j=1}^k n_j^\alpha}, \quad (8)$$

the second term of  $\Gamma_i$  can be approximated as

$$\frac{1}{1-\alpha} \ln \mathcal{D}_{\alpha,i} = \frac{1}{1-\alpha} (\mathcal{D}_{\alpha,i} - 1) + \mathcal{O}\left((\mathcal{D}_{\alpha,i} - 1)^2\right). \quad (9)$$

Let us note that the last term of Eq. (6) is nothing else than the THC entropy formula [4], [17]. In other words, at the condition of the utilization of the THC entropy instead of the Rényi entropy, it almost corresponds to the point information gain derived from Eq. (5). This is due to the fact that, for large  $n$ , the omission of the point have no large impact on the whole distribution. This refers to the fact that, for our purposes, the degree of the  $\alpha$ -parameter, which causes rescaling of probabilities to  $p_i^\alpha$ , is more important than the particular form of the information measure.

We shall continue utilizing Rényi entropy due to its correspondence to a generalized dimension of multifractal systems [18], [19]. Let us concentrate again to the term  $\mathcal{D}_{\alpha,i}$ . It can be rewritten as

$$\mathcal{D}_{\alpha,i} = \frac{\sum_{j=1}^k n_{j,i}^\alpha}{\sum_{j=1}^k n_j^\alpha} = \frac{\sum_{j=1, j \neq i}^{k-1} n_j^\alpha + (n_i - 1)^\alpha}{\sum_{j=1}^k n_j^\alpha} = 1 - \alpha \frac{n_i^{\alpha-1}}{\sum_{j=1}^k n_j^\alpha} + \frac{1}{\sum_{j=1}^k n_j^\alpha} \omega(n_i^{\alpha-2}). \quad (10)$$

Specifically, provided  $\alpha = 2$ , we obtain

$$\Gamma_{2,i} \approx \mathcal{C}_2(n) + \frac{1}{1-2} \left( \frac{\sum_{j=1, j \neq i}^{k-1} n_j^2 + (n_i - 1)^2}{\sum_{j=1}^k n_j^2} - 1 \right) \approx \mathcal{C}_2(n) + \frac{2n_i - 1}{\sum_{j=1}^k n_j^2}, \quad (11)$$

which explains why the dependency  $n_i$  on  $\Gamma_{2,i}$  is approximately linear (Fig. 2d). In general, if  $\alpha \neq 1$ , the point information gain is a monotonous function of  $n_i$ , respectively  $p_i$ , for all possible discrete distributions. Thus, it may be used as a measure of information gain between two discrete distributions, which in the occurrence of one particular feature differ.

In general,  $\Gamma_{\alpha,i} < 0$  correspond to tail parts of the distribution, which points to rare events, while  $\Gamma_{\alpha,i} > 0$  correspond to frequent events. Thus, in addition to definition of the measure of the contribution of each event to the examined distribution, we also obtain the discrimination between points which contribute to information about the given distribution under the given statistical assumption represented by the particular  $\alpha$ -value. This opens the question on existence of the so-called "optimal" distribution for the given  $\alpha$ . There naturally arise two possible measures of such optimality. The first one would be defined as a distribution for which exactly a half of the  $n_i$  values produces  $\Gamma_{\alpha,i} > 0$  and the other half yields  $\Gamma_{\alpha,i} < 0$ . The second one requires that  $\Gamma_{\alpha,i}$ -values are equally spaced. Existence of such an "ideal" distribution would be another generalization of the concept of the entropy power similar to that reported recently [20], [21]. We intend to address this question in our future research.

With respect to the previous discussion and practical utilization of this notion, we emphasize that for real systems with large  $n$ ,  $\Gamma_{\alpha,i}$ -values are rather small numbers. Their further computer averaging and numerical representation lead to significant errors (e.g., Fig. 1c). At lower  $\alpha$ -values, the  $\Gamma_{\alpha,i}$ -values are broadly separated for rare points, while at higher  $\alpha$ -values the resolution is higher for more frequent data points. Therefore,  $\Gamma_{\alpha,i}(\alpha)$ -spectrum is more advisable to compute, rather than a single  $\Gamma_{\alpha,i}$ -value at a chosen  $\alpha$ .

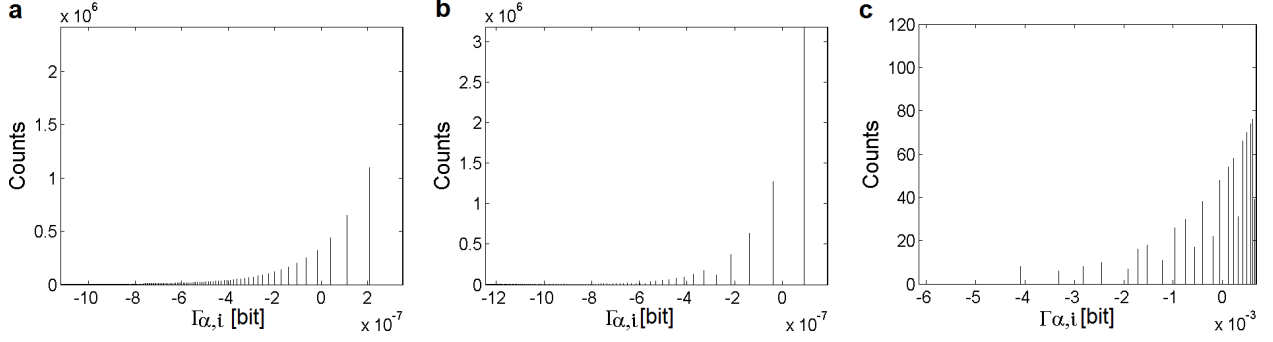


Fig. 1.  $\Gamma_{\alpha,i}$ -transformations of the discretized Lévy (a), Cauchy (b), and Gauss (c) distribution at  $\alpha = 0.99$ . The deviation from the monotonous dependency in the Gauss distribution is due to the digital rounding.

### B. Point information gain for typical distributions

In Fig. 1, we demonstrate  $\Gamma_{\alpha,i}$ -transformations of three thoroughly studied distributions – the Lévy, Cauchy, and Gauss distribution (specified in Sect. A-A). Digital level averaging which results in multiple appearance of unique points is observable there. This phenomenon is reduced with the increasing number of the points in the distribution, nevertheless, it does not disappear in any real case. Thus, the monotonous dependency of  $n_i$ , respectively  $p_i$ , on  $\Gamma_{\alpha,i}$  are valid only at the approximation to an infinite resolution in value levels.

Fig. 2 shows distribution changes of  $\Gamma_{\alpha,i}$ -values with the increasing  $\alpha$ -parameter. For each  $\alpha$ -parameter, the  $\Gamma_{\alpha,i}$ -elements are enveloped by monotonously increasing curves. For instance, as devised in Eq. (11), the near linearity of the dependency of the number of elements on  $\Gamma_{\alpha,i}$ -values at  $\alpha = 2$  is seen in Fig. 2d. The differences between distributions are expressed by the distributions of  $\Gamma_{\alpha,i}$ -values along the  $x$ -axes.

### C. Point information gain entropy and point information gain entropy density

During the previous sections, we showed that  $\Gamma_{\alpha,i}$  is different for any  $n_i$  and the dependency of these two variables is a monotonously increasing function for all  $\alpha > 0$ . Further, if  $\alpha > 0$ , the term  $\sum_{j=1}^k n_j^\alpha$  is different for any pair of dissimilar distribution classes. Here, we propose new variables – a point information gain entropy ( $H_\alpha$ ) and point information gain entropy density ( $\Xi_\alpha$ ) defined by formulae

$$H_\alpha = \sum_{j=1}^k n_j \Gamma_{\alpha,j} \quad (12)$$

and

$$\Xi_\alpha = \sum_{j=1}^k \Gamma_{\alpha,j}. \quad (13)$$

They can be understood as a multiple of the average point information gain and – under linear averaging – an average gain of the phenomenon  $j$ , respectively.

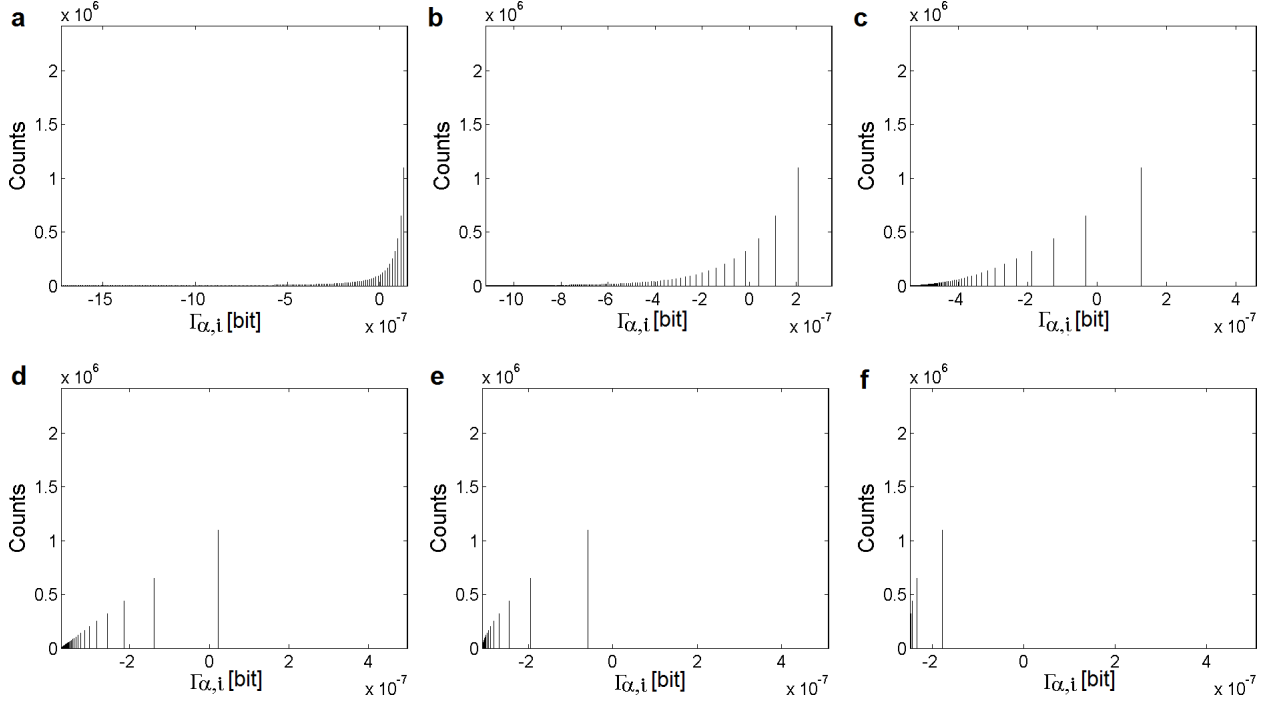


Fig. 2.  $\Gamma_{\alpha,i}$ -transformations of the discretized Lévy distribution at  $\alpha = \{0.5; 0.99; 1.5; 2.0; 2.5; 4.0\}$  (from **a** to **f**).

The information content is generally measured by the entropy. The famous Shannon source coding theorem [22] refers to a specific process of transmission of a discretized signal and introduction of the noise. The Rényi entropy is one of the class of one-parametric entropies and offers numerous additional features over the Shannon entropy [5], [10], [23], such as the determination of a generalized dimension of a strange attractor [18], [19]. The universality of the generalized dimension for characterization of any distribution, whose regularity may be only coincidental, is still under dispute. However, the  $H_\alpha$ - and  $\Xi_\alpha$ -values characterize unambiguously a given distribution for any  $\alpha$ . Differences between distributions are expressed in counts along the  $\Gamma_\alpha$ -axes. Thus, independently of the mechanism of its generation, the  $H_\alpha/\Xi_\alpha$ -value of the given distribution, also a non-parametric one, may be always compared.

The next question is whether  $\Xi_\alpha$  measures the information in a commonly understood way. In this aspect, we mention the fact observed upon examination of Eq. (9), i.e., that the point information gain  $\Gamma_{\alpha,i}$  has the properties of an information measure. We may rewrite it

$$\begin{aligned} \Xi_\alpha &= \sum_{j=1}^k \Gamma_{\alpha,j} = \frac{k}{1-\alpha} \ln \left( \frac{n^\alpha}{(n-1)^\alpha} \right) + \frac{1}{1-\alpha} \sum_{i=1}^k \ln \left( \frac{\sum_{j=1, j \neq i}^{k-1} n_j^\alpha + (n_i - 1)^\alpha}{\sum_{j=1}^k n_j^\alpha} \right) = \\ &= \mathcal{C}_\alpha(n) \cdot k + \frac{1}{1-\alpha} \ln \left( \prod_{j=1}^k \mathcal{D}_{\alpha,j} \right), \end{aligned} \quad (14)$$

where the product in the argument of the logarithm in the second term is a product of functions upper limited by 1 and thus again a function upper limited by 1. From the previous analysis done of  $\mathcal{D}_{\alpha,i}$ , we may conclude that the point information gain entropy density ( $\Xi_\alpha$ ) has properties of an information measure.

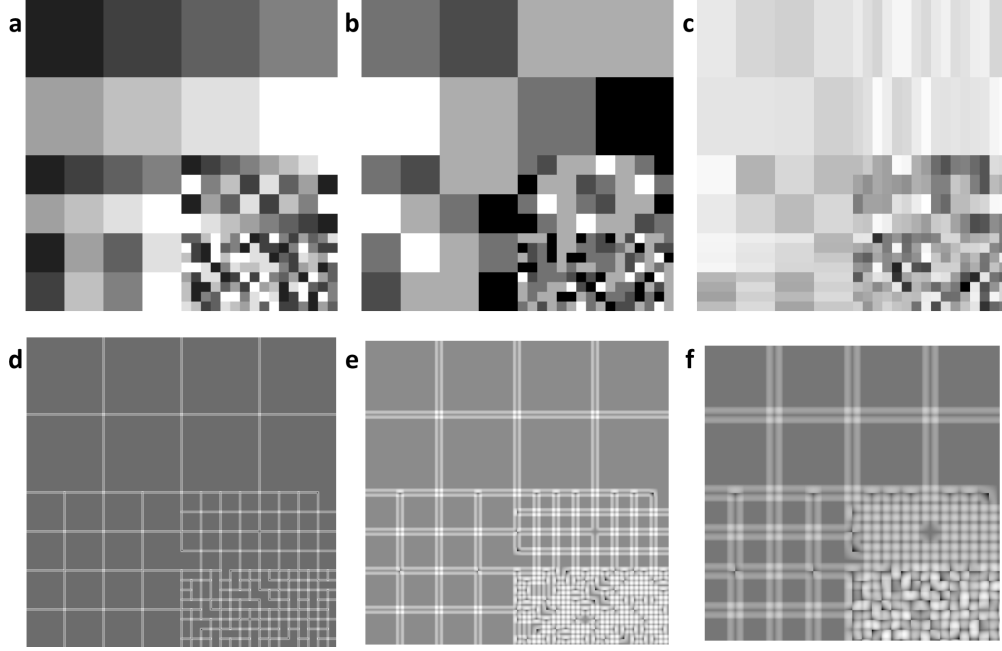


Fig. 3.  $\Gamma_{0.99,i}$ -transformations of the texmos2.s512 image [24]. Original image (a) and semantic information images calculated from the whole image (b), a cross around each pixel (c), and squares of the side of 5, 15, and 29 px, respectively, with the centered examined pixel (d-f).

Similarly, the point information gain entropy ( $H_\alpha$ ) may be rewritten to

$$\begin{aligned}
 H_\alpha &= \sum_{j=1}^k n_j \Gamma_{\alpha,j} = \frac{\sum_{j=1}^k n_j}{1-\alpha} \ln \left( \frac{n^\alpha}{(n-1)^\alpha} \right) + \sum_{i=1}^k n_i \ln \left( \frac{(\sum_{j=1, j \neq i}^{k-1} n_j^\alpha + (n_i - 1)^\alpha)}{\sum_{j=1}^k n_j^\alpha} \right) = \\
 &= C_\alpha(n) \cdot \sum_{j=1}^k n_j + \ln \left( \prod_{j=1}^k \mathcal{D}_{\alpha,j}^{n_j} \right). \quad (15)
 \end{aligned}$$

Again, the argument of the logarithm in the second term is upper limited by 1.  $H_\alpha$  has also properties of an information measure, although, in this case, its relation to the original Rényi entropy is more complicated.

### III. POINT INFORMATION GAIN, POINT INFORMATION GAIN ENTROPY, AND POINT INFORMATION GAIN ENTROPY DENSITY IN MULTIDIMENSIONAL DATASETS

#### A. Point information gain

Point information gain  $\Gamma_{\alpha,i}$  introduced in Eq. (5) was originally applied to an image enhancement [1], [2]. A typical digital image is a matrix of  $x \times y \times n$  values, where  $x$  and  $y$  are dimensions of the image and  $n$  corresponds to the number of color channels (e.g.,  $n$  is 1 and 3 for a monochrome and RGB image, respectively). In most cases, the intensity values are in the range from 0 to 255 (an 8-bit image) or from 0 to 4095 (a 12-bit image) for each color channel.

Nevertheless, independently of the size and bit depth of an image, we may also examine the context of each pixel in the image *via*  $\Gamma_{\alpha,i}$ -calculation. In other words, apart from the semantic information (Algorithm 1), the

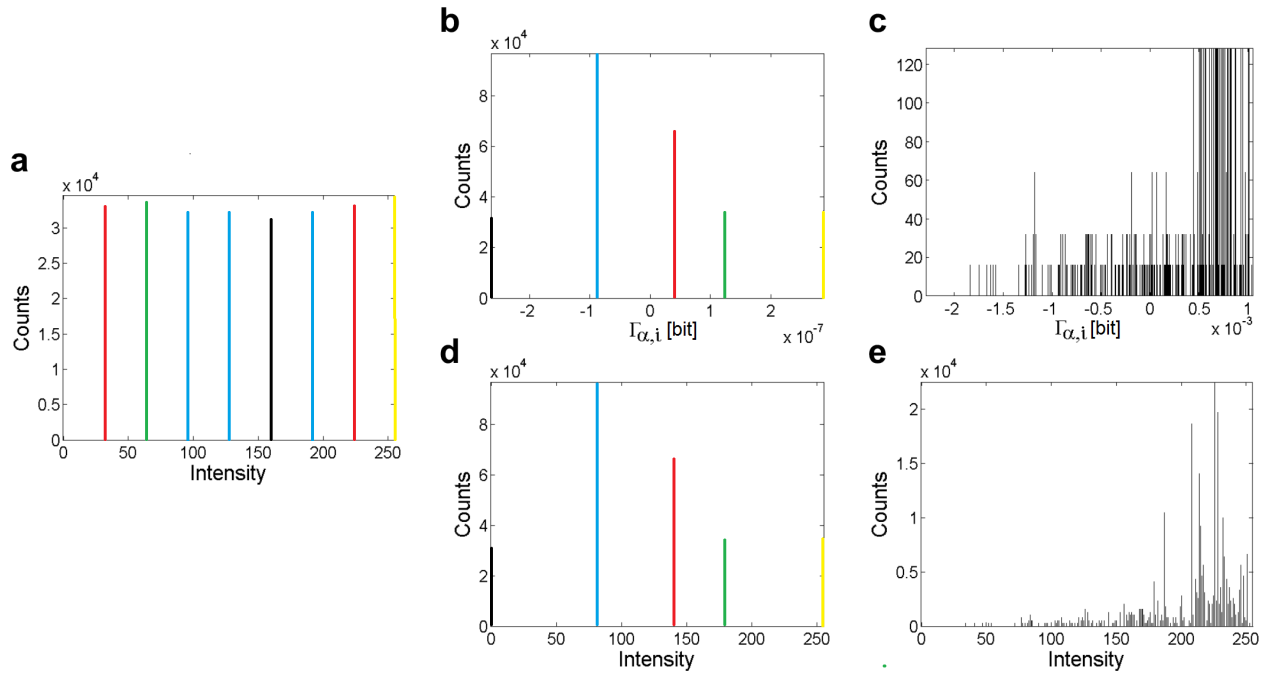


Fig. 4. Histograms of  $\Gamma_{0.99,i}$ -transformations of the texmos2.s512 image [24]. Original image (a), original  $\Gamma_{0.99,i}$ -values calculated from the whole image (b), original  $\Gamma_{0.99,i}$ -values calculated from a cross whose shanks intersect in the examined pixel (c),  $\Gamma_{0.99,i}$ -transformed images calculated from whole image (d), and  $\Gamma_{0.99,i}$ -transformed images calculated from a cross around each pixel (e). Colors in the original and globally (whole image) transformed histograms correspond to the intensity levels with the identical frequencies of occurrences in the original image.

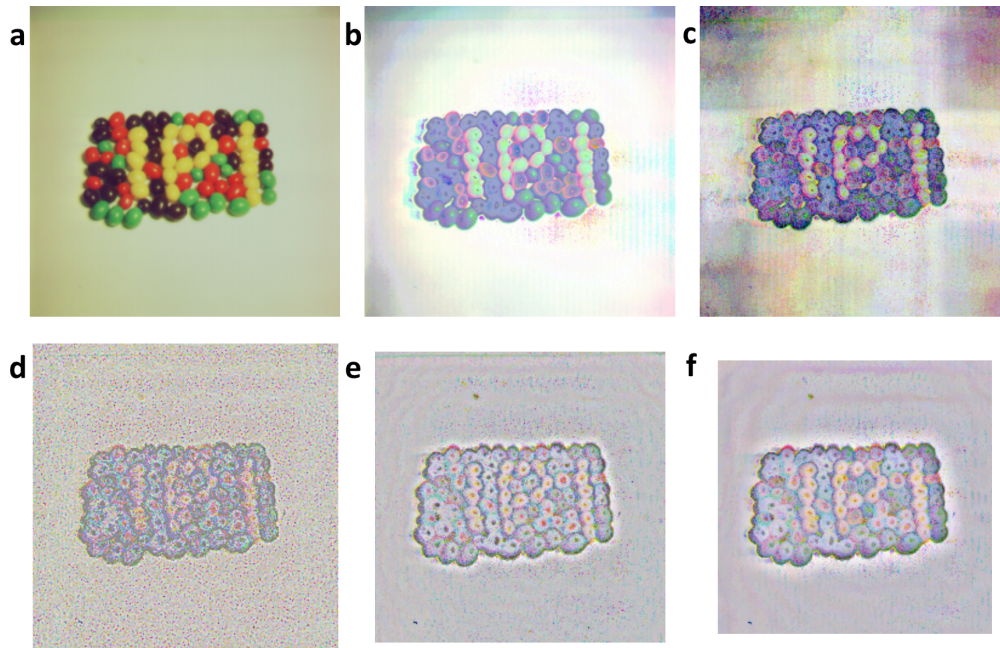


Fig. 5.  $\Gamma_{0.99,i}$ -transformations of the 4.1.07 image [24]. Original image (a) and semantic information images calculated from the whole image (b), a cross around each pixel (c), and circles of the diameter of 5, 17, and 30 px, respectively, with the centered examined pixel (d-f).

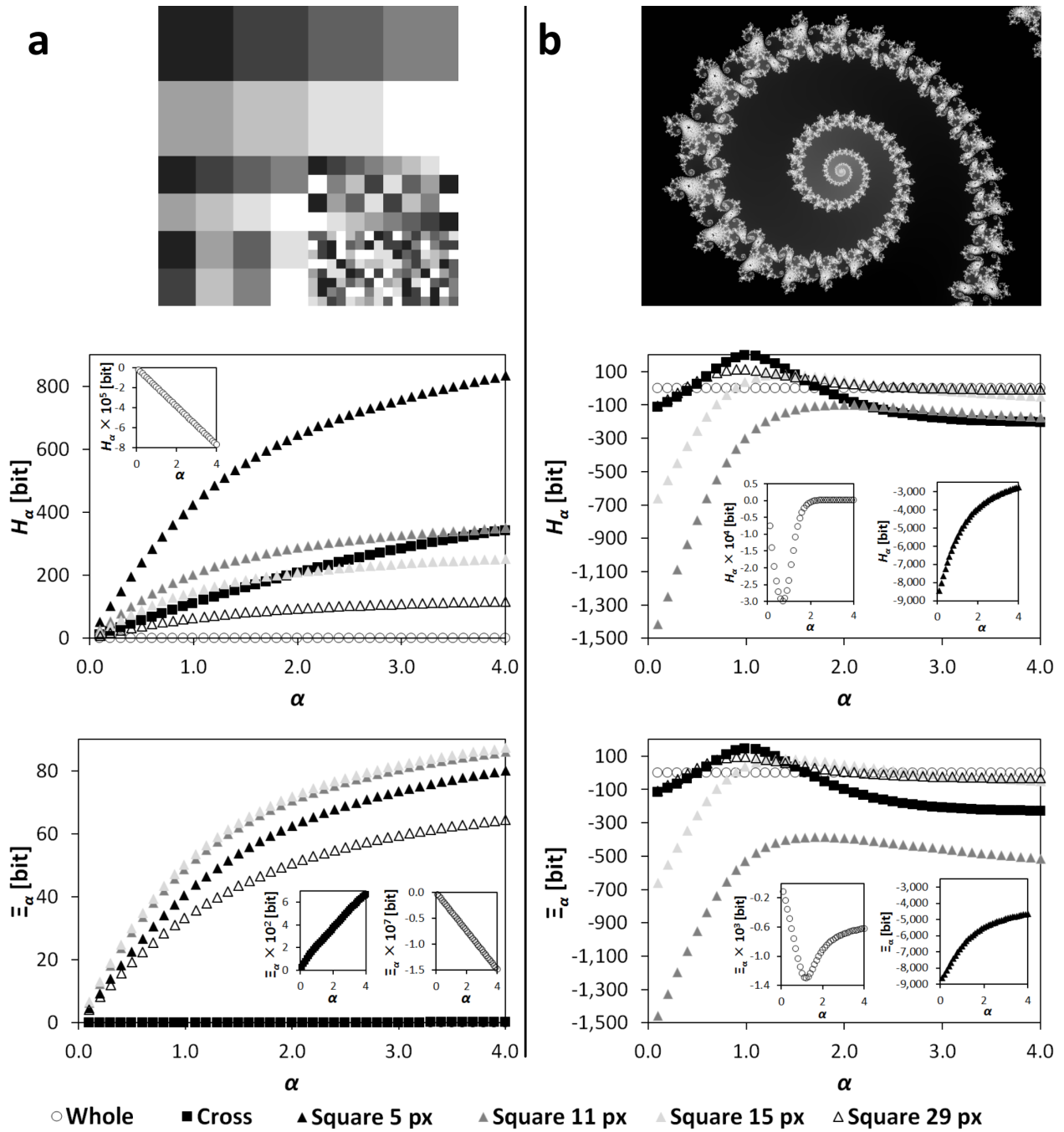


Fig. 6.  $H_\alpha$ - and  $\Xi_\alpha$ -spectra for semantic information and different syntactic surroundings of a unifractal (texmos2.s512 [24], column a) and multifractal (wd950112 [25], column b) image at  $\alpha = \{0.1, 0.2, \dots, 0.99, 1.1, 1.2, \dots, 4.0\}$ .

$\Gamma_{\alpha,i}$ -calculation also allows us to analyze syntactic information around each pixel (Algorithm 2). The semantic information is evaluated as a change of probability intensity histogram after removing a point at each occupied intensity level. The choice of the syntactic surroundings around pixels is specific for each image. According to our knowledge, the appropriate surroundings chosen on the basis of the origin of the image generation was, for the particular case of cellular automata, studied only in Refs. [26]–[28]. Thus, we do not have any systematic method for comparison of suitability of different definitions of surroundings of the pixels and it obviously depends on the process by which the observed pattern or other distribution was generated. This makes the study of the syntactic information very interesting, because it outlines the method of further discrimination of the processes of self-organization/pattern formation [29]. In this article, we confine ourselves on the usage of the syntactic information for better understanding both the limitation of the method of the  $\Gamma_{\alpha,i}$ -calculation and the syntactic information itself. The cross, square, and circle surroundings around each pixel are demonstrated on three different standard images – texmos2.s512 (monochrome, computer-generated, unifractal), 4.1.07 (RGB, photograph, unifractal) [24], and wd950112 (monochrome version, computer-generated, multifractal) [25].

For each parameter  $\alpha$ ,  $\Gamma_{\alpha,i}$ -calculation helps to find values of the intensities with the identical occurrences and determine their distribution in (a structural part of) the image. Thus, in general, the  $\Gamma_{\alpha,i}$ -recalculations can be considered as Look-up Tables – intensities with the highest probabilities of occurrences in an image correspond to the highest (positive)  $\Gamma_{\alpha,i}$ -values and the brightest intensities in a  $\Gamma_{\alpha,i}$ -transformed image and *vice versa*. Sometimes, mainly in case of syntactic information, due to the transformation of the original  $\Gamma_{\alpha,i}$ -values into an 8-bit resolution, some  $\Gamma_{\alpha,i}$ -levels are merged into one intensity level of the transformed image.

Everything is best visualized in Figs. 3–4 which show the  $\Gamma_{\alpha,i}$ -transformations of the texmos2.s512 image. Its creator’s intention has been probably to make an image with a uniform distribution of intensities. Provided the uniform intensity distribution, the output of the global  $\Gamma_{\alpha,i}$ -calculation would be only one  $\Gamma_{\alpha,i}$ -value, i.e., Fig. 3b would be unicolor. However, 8 original intensities (Fig. 3a) resulted in five  $\Gamma_{0.99,i}$ -values (i.e., syntactic parts) (Fig. 4b,d). The detailed image analysis showed that the number of occurrences is only identical for intensities 32-224 and 96-128-192, i.e., there are five unique values of frequencies of intensity occurrences (Fig. 4a). For a change, in the 4.1.07 image, the global (semantic)  $\Gamma_{0.99,i}$ -recalculation emphasizes the unevenness of the background and shadows around a group of the jelly beans (Fig. 5b). In conformity with the statement in the next-to-last paragraph of Sect. II-A, this principle also enables to highlight rare points in much more intensity richer images, mainly at low  $\alpha$ -values. The calculations using higher  $\alpha$ -values merge resulted  $\Gamma_{\alpha,i}$ -values and draw areas.

The syntactic information emphasizes differences based on a local concept. The cross from the intensity values, whose shanks meet in the examined point of the original image [1], was chosen as the first syntactic surroundings. In contrast to the global (semantic) recalculation, such a transformation of the texmos2.s512 image produces a substantially much intensity richer  $\Gamma_{\alpha,i}$ -image. One can see that a relatively simple semantic information consists of a more complex syntactic information (Fig. 4a,c,e).

However, the cross-syntactic type of the image transformation is the least suitable approach for the analysis of the photograph of the jelly beans (Fig. 5c). In this case, a circle syntactic element is rather recommended to use. As seen in Figs. 5d–f, increase of the circle diameter up to the size of the jelly beans reduces the background

gradually. The next increase enables to group the jelly beans into higher-order assemblies. A similar grouping is observable for the smallest squares in the transformed `texmos2.s512` using the 29-px square surroundings (Fig. 3f). In contrast, lower values of square surroundings (Fig. 3d) highlight only the intensity borders.

### B. Point information gain entropy and point information gain entropy density

From the point of view of thermodynamics,  $H_\alpha$  and  $\Xi_\alpha$  can be considered as additive, homological, state variables and their knowledge can be also helpful in analysis of multidimensional (image) data [30]. Despite the relative familiarity of their formulae (Sect. II-C),  $H_\alpha$  can be defined as a sum of all information contributions to the data distribution, either the global or partial one, i.e., all  $\Gamma_{\alpha,i}$ , whereas  $\Xi_\alpha$  is a sum of all information microstates of the distribution. Even, in case of the syntactic information, each of two (collision) histograms with the same proportional representation of frequencies of elements, which were obtained from distributions around two pixels at the different positions and only in the positions of frequencies in the histogram differ, are considered to be unique microstates and produce unique  $\Gamma_{\alpha,i}$ -values (see Algorithm 2). Thus, in agreement with the predictions arising from Eqs. (12)–(13),  $\Xi_\alpha$ -calculation does not suppress contributions of elements with a low probabilities of occurrences (rare points) and is more robust and stable to changes in the syntactic surroundings. This phenomenon manifests itself in the lower differences in  $\Xi_\alpha(\alpha)$ -dependences for four square surroundings in comparison to  $H_\alpha(\alpha)$ -courses in Fig. 6. Nevertheless, it is worth noting that, during the calculation with the usage of the syntactic geometrical surroundings, the surroundings touch the edges of the image at the most and an interior part of the image is only processed. This fact – technical limitation – negatively influences  $H_\alpha$ - and  $\Xi_\alpha$ -values for square surroundings in Fig. 6 and also leads to the lower sizes of  $\Gamma_{\alpha,i}$ -transformed images (e.g., Figs. 3d–f and 5d–f).

Plotting  $H_\alpha$  and  $\Xi_\alpha$  vs.  $\alpha$  in Fig. 6 is not random. Similarly as mentioned for  $\Gamma_{\alpha,i}$ -calculations (Sect. II-A), multidimensional discrete (image) data is suitable to characterize not only by one discrete value, either  $H_\alpha$  or  $\Xi_\alpha$ , at a particular  $\alpha$ , but also by their  $\alpha$ -dependent spectra. The reason is not only to avoid digital rounding, but, as written in Sect. III-A, there is also a possibility to characterize the type and origin of geometrical structures in the image. Another application is in the statistical evaluation of the time-lapse multidimensional datasets [30]. This calculation method was originally developed for study of multifractal self-organizing biological images [31], [32], however, it enables to describe any types of images. Since parts of an image are forms of complex structures, the best way how to interpret the image is to use a combination of its semantic and syntactic kinds of information. We demonstrate that in Fig. 6, which contains an example of a unifractal (almost non-fractal) Euclidian image and a computer-generated multifractal image. Whereas the Euclidian image gives monotonous  $H_\alpha/\Xi_\alpha(\alpha)$ -spectra (for the semantic and cross-syntactic kinds of information, even almost linear dependences at the particular discrete interval of  $\alpha$ -values), the recalculation of the multifractal image shows extremes at values of  $\alpha$  close to 1. Analogous dependences have been also plotted for the image sets of the course of the self-organizing Belousov-Zhabotinsky reaction [30].

## IV. CONCLUSIONS

In this article, we propose novel information measures – a point information gain ( $\Gamma_{\alpha,i}$ ), a point information gain entropy ( $H_\alpha$ ), and a point information gain entropy density ( $\Xi_\alpha$ ). Variables  $H_\alpha$  and  $\Xi_\alpha$  may be used as measures in multidimensional datasets for the definition of the information context. This option may be practically utilized for acquisition of differently resolved information measures in a dataset. In other words, it enables to avoid cases, where the number of occurrences of a certain event is the same, but in distribution in time, space or along any other measure differ. Examination of syntactic information distribution shows a potential for in-depth insight into formation of observed structures and patterns. Further, we found a monotonous dependency of the number of the elements of a given property in the set on  $\Gamma_{\alpha,i}$ . In principle, variables  $H_\alpha$  and  $\Xi_\alpha$  are unique for each distribution but suffer from problems with digital precision of the calculation. Therefore, we proposed the  $\Gamma_{\alpha,i}$ -spectrum as a proper characteristics of any discrete distribution.

## APPENDIX A

## MATERIALS AND METHODS

## A. Processing of images and typical histograms

$\Gamma_{\alpha,i}$ -,  $H_\alpha$ -, and  $\Xi_\alpha$ -values for all typical histograms and images were computed using Eqs. (5), (12), and (13). Algorithms are described in Sect. A-B. The software and scripts, as well as results of all calculations are available as written in Sect. B.

For the Cauchy, Lévy, and Gauss distributions, histograms of dependences of the number of elements on  $\Gamma_{\alpha,i}$ -values were calculated for  $\alpha = \{0.1, 0.3, 0.5, 0.7, 0.99, 1.3, 1.5, 1.7, 2.0, 2.5, 3.0, 3.5, 4.0\}$  using a Matlab<sup>®</sup> script (Mathworks, USA). The following probability density functions  $f(x)$  were studied:

a) Lévy distribution:

$$f(x) = \text{round} \left[ 10^c \frac{\exp(-\frac{1}{2x})}{\sqrt{2\pi x^3}} \right], \quad x \in \langle 1, 256 \rangle, \quad x \in \mathbb{N}, \quad c \in \{3, 5, 7\}, \quad (16)$$

b) Cauchy distribution:

$$f(x) = \text{round} \left[ 10^c \frac{1}{\pi(1+x^2)} \right], \quad x \in \langle -127, 127 \rangle, \quad x \in \mathbb{Z}, \quad c \in \{3.5, 7\}, \quad (17)$$

c) Gauss distribution:

$$f(x) = \text{round} \left[ 10^c \frac{\exp(-\frac{x^2}{2\sigma^2})}{\sigma\sqrt{2\pi}} \right], \quad x \in \langle -127, 127 \rangle, \quad x \in \mathbb{Z}, \quad c \in \{4, 300\} \wedge \sigma = 1, \quad c \in \{3, 4\} \wedge \sigma = 10. \quad (18)$$

In Figs. 1–2, the Cauchy and Lévy distributions with  $c = 7$  and the Gauss distribution with parameters  $c = 4$  and  $\sigma = 10$  are depicted.

Multidimensional image analysis based on calculation of  $\Gamma_{\alpha,i}$ ,  $H_\alpha$ , and  $\Xi_\alpha$  was tested on 5 standard images (Table I). Before the computations, original images wd950112.gif and 6ASCP011.gif obtained from [25] were transformed into monochrome \*.png formats in Matlab<sup>®</sup> software. All images were processed using an Image Info Extractor Professional software (Institute of Complex System, FFPW, USB, Czech Republic) for  $\alpha = \{0.1, 0.2,$

TABLE I  
SPECIFICATIONS OF IMAGES.

Image	source	bit-depth/colors	resolution	geometry	origin
texmos2.s512.png	[24]	8-bit/gray	512×512	unifractal	computer-based
4.1.07.tiff	[24]	24-bit/RGB	256×256	unifractal	photograph
wash-ir.tiff	[24]	24-bit/RGB	2250×2250	unifractal	computer-based
wd950112.png	[25]	8-bit/gray	1024×768	multifractal	computer-based
6ASCP011.png	[33]	8-bit/gray	1600×1200	multifractal	computer-based

..., 0.9, 0.99, 1.1, 1.2, ..., 4.0}. The semantic information was extracted using<sup>4</sup> *Whole Image* calculation. The vertical-horizontal cross, square (a side of 5, 11, 15, and 29 px, respectively), and circle (a radius of 2, 5, and 8 px, respectively) syntactic information was set as special cases of a *Cross*, *Rectangle*, and *Ellipse* calculation at the rotation angle  $\Phi$  of 0°. Into the Image Info Extractor Professional software, a side of the square and radius of the circle surroundings is inputted as *width/2* and *height/2* of 2, 5, and 14 px and *a* and *b* of 2, 5, and 8 px, respectively.

### B. Calculation algorithms

The algorithms implemented into the Image Info Extractor Professional are described in Algorithms 1–2. In case of RGB images, the algorithms were applied to each color channel. The  $\Gamma_{\alpha,i}$ -values were visualized by a full rescaling into 8-bit resolution. Let us note that, for  $\alpha = 1$ , the equations in lines 9 of the both algorithms switch to the calculation of the Shannon entropy.

## APPENDIX B SUPPLEMENTARY DATA

All processed data are available at [34] (for more details, see Sect. A):

- 1) Folder "Figures" contains subfolders with results of  $\Gamma_{\alpha,i}$ -,  $H_{\alpha}$ -, and  $\Xi_{\alpha}$ -calculations for "RGB" (4.1.07.tiff, wash-ir.tiff) and "gray" (texmos2.s512.png, wd950112.png, 6ASCP011.png) standard images calculated for 40  $\alpha$ -values. The results are separated into subfolders according to the type of extracted information.
- 2) Folder "H\_Xi" stores the PIE\_PIED.xlsx and PIE\_PIED2.xlsx files with dependences of  $H_{\alpha}$  and  $\Xi_{\alpha}$  on  $\alpha$  as exported from the PIE.mat files (in folder "Figures"). Titles of the graphs, which are in agreement with the computed variables and extracted kinds of information, are written in the sheets.
- 3) Folder "Histograms" stores the histograms of the occurrences of  $\Gamma_{\alpha,i}$ -values for the Cauchy (2 types), Lévy (3 types), and Gauss (4 types) distributions. The parameters of the original distributions are saved in the equation.txt files. All histograms were recalculated using 13  $\alpha$ -values.

<sup>4</sup>The italics refer to parameters which are set in the Image Info Extractor Professional software.

**Input:**  $n$ -bin histogram  $\mathbf{h}$ ;  $\alpha$ , where  $\alpha \geq 0 \wedge \alpha \neq 1$

**Output:**  $\Gamma_\alpha$ ;  $H_\alpha$ ;  $\Xi_\alpha$

```

1  $\mathbf{p} = \mathbf{h}/\text{sum}(\mathbf{h})$ ;      % explain the frequency histogram  $\mathbf{h}$  as a probability histogram  $\mathbf{p}$ 
2  $\Gamma_\alpha = \text{zeros}(\mathbf{h})$ ;    % create a zero matrix  $\Gamma_\alpha$ 

3 for  $i = 1$  to  $n$  do
4      $\mathbf{h}_2 = \mathbf{h}$ ;      % create a vector  $\mathbf{h}_2$  identical to the histogram  $\mathbf{h}$ 
5     if  $\mathbf{h}_2(i) \neq 0$  then
6          $\mathbf{h}_2(i) = \mathbf{h}_2(i) - 1$ ;
7         % if the bin  $i$  of the histogram  $\mathbf{h}_2$  is occupied, remove an element at the position  $i$ 
8     end
9      $\mathbf{p}_2 = \mathbf{h}_2/\text{sum}(\mathbf{h}_2)$ ;    % calculate a probability histogram  $\mathbf{p}_2$  without the examined element
10     $\Gamma_\alpha(i) = \frac{1}{1-\alpha} \log_2(\text{sum}(\mathbf{p}_2.^{\alpha})/\text{sum}(\mathbf{p}.^{\alpha}))$ ;
11    % calculate  $\Gamma_{\alpha,i}$  as a difference of two Rényi entropies – with and without the examined element,
12    % respectively Eq. (5))
13 end

14  $H_\alpha = \text{sum}(\mathbf{h}.*\Gamma_\alpha)$ ;
15 % calculate  $H_\alpha$  as a sum of the element-by-element multiplication of  $\mathbf{h}$  and  $\Gamma_\alpha$  (Eq. (12))
16  $\Xi_\alpha = \text{sum}(\Gamma_\alpha)$ ;    % calculate  $\Xi_\alpha$  as a sum of all unique values in  $\Gamma_\alpha$  (Eq. (13));

```

**Algorithm 1:** Point information gain vector ( $\Gamma_\alpha$ ), point information gain entropy ( $H_\alpha$ ), and point information gain entropy density ( $\Xi_\alpha$ ) calculations for semantic (Whole image) information and typical histograms.

4) Folder "Software" contains a 32- and 64-bit version of an Image Info Extractor Professional v. b9 software (ImageExtractor\_b9\_  $xx$  bit.zip; supported by OS Win7) and a pig\_histograms.m Matlab<sup>®</sup> script for recalculation of the typical probability density functions. Script pie\_ec.m serves for the extraction of  $H_\alpha$  and  $\Xi_\alpha$  from the folders (outputs from the Image Info Extractor Professional) over  $\alpha$ . In the software and script, the  $\Gamma_{\alpha,i}$ -,  $H_{\alpha}$ -, and  $\Xi_{\alpha}$ -variables are called *PIG*, *PIE*, and *PIED*, respectively. Manuals for the software and scripts are also attached.

**Input:** 2-D discrete data  $\mathbf{I}_{m \times n}$ ;  $\alpha$ , where  $\alpha \geq 0 \wedge \alpha \neq 1$ ; parameters of surroundings  $a, b$

**Output:**  $\Gamma_{\alpha, i}$ ;  $H_{\alpha}$ ;  $\Xi_{\alpha}$

```

1  $\Gamma_{\alpha} = \text{zeros}(\mathbf{I});$       % create a zero matrix  $\Gamma_{\alpha}$  of the size of the  $\mathbf{I}_{m \times n}$  matrix
2 hashMap = containers.Map;    % declare an empty hash-map (the key-value array)

3 for  $i = (a + 1)$  to  $(m - a - 1)$  do
4   for  $j = (b + 1)$  to  $(n - b - 1)$  do
5      $\mathbf{h} = \text{getHist}(\mathbf{I}(i, j));$     % create a histogram  $\mathbf{h}$  from the elements around the pixel  $(i, j)$  of  $\mathbf{I}_{m \times n}$ 
6      $\mathbf{p} = \mathbf{h}/\text{sum}(\mathbf{h});$     % explain histogram  $\mathbf{h}$  as a probability histogram  $\mathbf{p}$ 
7      $\mathbf{h}(\mathbf{I}(i, j)) = \mathbf{h}(\mathbf{I}(i, j)) - 1;$     % remove the examined point  $(i, j)$  from the histogram  $\mathbf{h}$ 
8      $\mathbf{p}_2 = \mathbf{h}/\text{sum}(\mathbf{h});$     % explain the histogram  $\mathbf{h}$  as a probability histogram  $\mathbf{p}_2$ 
9      $\Gamma_{\alpha}(i, j) = \frac{1}{1-\alpha} \log_2(\text{sum}(\mathbf{p}_2.^{\alpha})/\text{sum}(\mathbf{p}.^{\alpha}));$ 
    % calculate  $\Gamma_{\alpha, i, j}$  as a difference of two Rényi entropies – with and without the examined element
     $(i, j)$  (Eq. (5))

10     $v = \mathbf{I}(i, j);$     % read a value of the element (intensity) at the position  $\mathbf{I}(i, j)$ 
11     $\text{checkSum} = \text{calcCheckSum}(\mathbf{h}, v);$ 
    % calculate  $\text{checkSum}$  using a hash-function effective enough (MD4, MD5, SHA1,...)

12    if not hashMap.isKey( $\text{checkSum}$ ) then
13       $\text{hashMap}(\text{checkSum}) = \Gamma_{\alpha}(i, j);$ 
      % if the hash-map does not contain the key, insert a new element with the key  $\text{checkSum}$ ,
      % where the inserted value is the  $\Gamma_{\alpha}$  for the element  $\mathbf{I}(i, j)$ 
14    end
15  end
16 end

17  $H_{\alpha} = \text{sum}(\text{sum}(\Gamma_{\alpha}));$     % calculate  $H_{\alpha}$  as a sum of all elements in the matrix  $\Gamma_{\alpha}$  (Eq. (12))
18  $\Xi_{\alpha} = \text{sum}(\text{values}(\text{hashMap}));$     % calculate  $\Xi_{\alpha}$  as a sum of all elements in the matrix hashMap
    (Eq. (13))

```

**Algorithm 2:** Point information gain matrix ( $\Gamma_{\alpha}$ ), point information gain entropy ( $H_{\alpha}$ ), and point information gain entropy density ( $\Xi_{\alpha}$ ) calculations for syntactic kinds of information. Parameters  $a$  and  $b$  are semiaxes of the ellipse surroundings and a half-width of the rectangle surroundings, respectively,  $a = 0$  and  $b = 0$  for the cross surroundings.

## REFERENCES

- [1] D. Štys, J. Urban, J. Vaněk, and P. Císař, “Analysis of biological time-lapse microscopic experiment from the point of view of the information theory,” *Micron*, vol. 42, pp. 3360–365, 2010.
- [2] J. Urban, J. Vaněk, and D. Štys, “Preprocessing of microscopy images via shannon’s entropy,” in *Proceedings of Pattern Recognition and Information Processing, Minsk, Belarus*, 2009, pp. 183–187.
- [3] P. T. D. Boer, D. Kroese, S. Mannor, and R. Rubinstein, “A tutorial on the cross-entropy method,” *Ann. Oper. Res.*, vol. 134, 2002.
- [4] C. Tsallis, “Possible generalization of boltzmann-gibbs statistics,” *J. Stat. Phys.*, vol. 52, pp. 479–487, 1988.
- [5] P. Jizba and T. Arimitsu, “The world according to rényi: Thermodynamics of multifractal systems,” *Ann. Phys.*, vol. 312, pp. 17–59, 2004.
- [6] P. Jizba and J. Korbel, “Multifractal diffusion entropy analysis: Optimal bin width of probability histograms,” *Phys. A*, vol. 413, pp. 438 – 458, 2014.
- [7] H. Hentschel and I. Procaccia, “The infinite number of generalized dimensions of fractals and strange attractors,” *Phys. D*, vol. 88, pp. 435–444, 1985.
- [8] L. L. Campbell, “A coding theorem and rényi’s entropy,” *Information and Control*, vol. 8, no. 4, pp. 423–429, 1965.
- [9] D. Štys, P. Jizba, S. Papáček, T. Náhlík, and P. Císař, “On measurement of internal variables of complex self-organized systems and their relation to multifractal spectra,” in *IWSOS 2012*, P. H. F.A. Kuipers, Ed. Springer, Berlin and Heidelberg, 2012, pp. 36–47.
- [10] A. Rényi, “On measures of entropy and information,” *Proc. Fourth Berkeley Symp. on Math. Statist. and Prob.*, vol. 1, pp. 547–561, 1961.
- [11] S. Kullback and R. Leibler, “On information and sufficiency,” *Ann. Math. Stat.*, vol. 22, pp. 79–86, 1951.
- [12] I. Csiszár, “I-divergence geometry of probability distributions and minimization problems,” *Ann. Prob.*, vol. 3, pp. 146–158, 1975.
- [13] P. Harremoës, “Interpretations of rényi entropies and divergences,” *Phys. Stat. Mech. Appl.*, vol. 365, pp. 5–62, 2006.
- [14] T. van Erven and P. Harremoës, “Rényi divergence and kullback-leibler divergence,” *IEEE Trans Inf Theory*, vol. 60, no. 7, pp. 3797–3820, 2014.
- [15] T. van Erven and P. Harremoës, “Rényi divergence and majorization,” in *Information Theory Proceedings (ISIT), 2010 IEEE International Symposium on*. IEEE, 2010, pp. 1335–1339.
- [16] P. Jizba, H. Kleinert, and M. Shefaat, “Rényi’s information transfer between financial time series,” *Phys. A*, vol. 391, pp. 2971–2989, 2012.
- [17] J. Havrda and F. Charvát, “Quantification method of classification processes. concept of structural  $\alpha$ -entropy,” *Kybernetika*, vol. 3, pp. 30–35, 1967.
- [18] P. Grassberger and I. Procaccia, “Measuring the strangeness of strange attractors,” *Phys. D*, vol. 9, pp. 189–208, 193.
- [19] —, “Characterization of strange attractors,” *Phys. Rev. Lett.*, vol. 50, pp. 346–349, 1983.
- [20] M. H. Costa, “A new entropy power inequality,” *IEEE Trans. Inform. Theory*, vol. 31, pp. 751–760, 1985.
- [21] P. Jizba, J. A. Dunningham, and J. Joo, “Role of information theoretic uncertainty relations in quantum theory,” *Ann. Phys.*, vol. 355, pp. 87 – 115, 2015.
- [22] C. E. Shannon, “A mathematical theory of communication,” *Bell Syst. Tech. J.*, vol. 27, pp. 379–423, 1948.
- [23] P. Jizba and T. Arimitsu, “On observability of rényi’s entropy,” *Phys. Rev. E*, vol. 69, p. 026128, 2004.
- [24] <http://sipi.usc.edu/database/database.php?volume=textures&image=61#top>.
- [25] <https://www.pinterest.com/pin/254031235202385248/>.
- [26] C. R. Shalizi and J. P. Crutchfield, “Computational mechanics: Pattern and prediction, structure and simplicity,” *J. Stat. Phys.*, vol. 104, no. 3–4, pp. 817–879, 2011.
- [27] C. R. Shalizi and K. L. Shalizi, “Quantifying self-organization in cyclic cellular automata,” in *SPIE’s First International Symposium on Fluctuations and Noise*. International Society for Optics and Photonics, 2003.
- [28] C. R. Shalizi, K. L. Shalizi, and R. Haslinger, “Quantifying self-organization with optimal predictors,” *Phys. Rev. Lett.*, vol. 93, p. 118701, 2004.
- [29] J. P. Crutchfield, “Between order and chaos,” *Nature Physics*, vol. 8, pp. 17–24, 2012.
- [30] A. Zhyrova, D. Štys, and P. Císař, “Macroscopic description of complex self-organizing system: Belousov-zhabotinsky reaction,” in *ISCS 2013*, ser. Emergence, Complexity and Computation, A. S. et al., Ed., vol. 8. Springer-Verlag, Berlin Heidelberg, Germany, 2014, pp. 109–115.
- [31] D. Štys, J. Urban, J. Vaněk, and P. Císař, “Analysis of biological time-lapse microscopic experiment from the point of view of system theory,” *Micron*, vol. 7, pp. 360–365, 2011.

- [32] D. Štys, J. Vaněk, T. Náhlík, J. Urban, and P. Císař, "The cell monolayer trajectory from the system state point of view," *Molecular BioSystems*, vol. 42, no. 10, pp. 2824–2833, 2011.
- [33] <http://cims.nyu.edu/~kiryl/Photos/Fractals1/ascp011et.html>.
- [34] <ftp://160.217.215.251/pig> (user: anonymous; password: anonymous).